

# Chitosan-genipin nanohydrogel as a vehicle for sustained delivery of alpha-1 antitrypsin

Ahmad Ghasemi<sup>1\*</sup>, Mahnaz Mohtashami<sup>2</sup>, Samaneh Sotoudeh Sheijani<sup>3</sup>, and Kamelya Aliakbari<sup>4</sup>

<sup>1</sup>Department of Clinical Biochemistry, Faculty of Medical Sciences, Tarbiat Modares University, Tehran, I.R. Iran

<sup>2</sup>Department of Microbiology, Alzahra University, Tehran, I.R. Iran.

<sup>3</sup>Department of Biochemistry, Payam Noor University, Tehran, I.R. Iran.

<sup>4</sup>Medical Biotechnology, School of Medicine, Flinders University, Adelaide, Australia.

---

## Abstract

Alpha-1antitrypsin (A1AT) deficiency, an inherited disorder, has been shown to be the cause of lung diseases such as emphysema and chronic obstructive pulmonary disease. One of the treatment strategies to provide appropriate and adequate concentrations of A1AT in the lungs is the application of nanoparticles (NPs) in pulmonary drug delivery. In the current study, biocompatible nanohydrogels were prepared using chemically cross-linked chitosan with genipin, a natural cross linker reagent, and used as a carrier to deposit A1AT into the lung tissue. Colloidal and monodispersed NPs were synthesized through reverse microemulsion. Nanohydrogels were characterized with TEM, DLS, FTIR, ZETA potential, UV spectrum, and swelling test. Encapsulation efficacy was determined at different concentrations of A1AT using Bradford assay. Effect of processing variables such as pH, loading efficiency, and release media components on drug release profile was determined in simulated lung fluids. To evaluate the inhibitory activity of the A1AT after release from NPs, trypsin inhibitory capacity assay was carried out. Results from FTIR and UV spectrum confirmed the development of chitosan cross linkage. Spherical chitosan-genipin NPs were sized from 30-100 nm. NPs exhibited the ability to release 49% of the drug within 12-day period at pH 7. However, there were variations with the drug release profile due to pH variations and loading efficacy. Drug release was higher in pseudo alveolar fluid in comparison with saline solution. These data indicate that application of chitosan nanohydrogels can be a useful tool for sustained release of A1AT in the lung tissue.

**Keywords:** Alpha-1antitrypsin; Chitosan; Genipin; Nanohydrogel; Simulated lung fluids; Drug delivery

---

## INTRODUCTION

Alpha-1 antitrypsin (A1AT) is a 54 kDa glycoprotein which belongs to the serpin super family. It is known as the human neutrophil elastase inhibitor protecting the lungs from human neutrophil elastase activity. In the absence of A1AT, neutrophil elastase secreted by the lung macrophages is not inhibited leading to elastin breakdown and loss of lung elasticity. This causes degradation of the lung tissue resulting in pulmonary complications such as emphysema or chronic obstructive pulmonary disease (COPD) in adults (1-4). Therefore, the lung normal functions can be maintained only with appropriate and adequate concentrations of A1AT. There are different

strategies to overcome lung A1AT deficiency which include replacement therapy using intravenous infusion or pulmonary delivery of aerosolized A1AT. In drug delivery through the airways not only the protein directly reaches the target sites but also prevents the accumulation of excess drug in the blood and therefore a much lower level of drug is required (5-8). Hydrogels are cross-linked polymeric particles composed of water-soluble and swellable polymer chains. They are safe, nontoxic and biodegradable polymeric networks with three-dimensional configuration capable of imbibing high amounts of water or biological fluids. The tunable chemical and physical structure, mechanical properties, high water content, and biocompatibility of

---

\*Corresponding author: A. Ghasemi  
Tel: 0098 514 3338381, Fax: 0098 514 3343474  
Email: ghasemi.a51@gmail.com

hydrogels have sparked particular interest in their use in drug delivery applications. There are several advantages for polymer-based drug delivery systems such as interior network for the incorporation of biocompatible, large surface area for different kind of bioconjugates, and capacity of preparation of particles in tunable size from nanometers to micrometer (9-12).

In recent years, chitosan has been widely used in the field of drug delivery owing to its biocompatibility, biodegradation, non-immunogenicity, mucoadhesiveness and absorption enhancing activity with great safety (10).

The cross-linked chitosan swells under acidic conditions due to protonation of their free amino groups and the expansion of matrix due to the electrostatic repulsion among these positively charged groups. These events increase entrance of water and water-soluble drugs to the hydrogel network (9,13,14). Degree of repulsion, swelling, and water absorption are also relative to the type and amount of cross linker. Several cross-linkers such as glutaraldehyde (15), tripolyphosphate (16) and genipin (11) are extensively used for particle formation.

The use of natural cross-linkers to prepare nanohydrogels has become a promising alternative to prepare fully biocompatible materials. genipin, a natural cross-linker, is obtained from geniposide from the fruits of *Gardenia jasminoides* Ellis (11,17,18). Toxicity of genipinis approximately 10,000 times less than glutaraldehyde (19).

In this study, we prepared chitosan-based nanohydrogel using genipin, a natural and biocompatible molecule as cross-linker by reverse microemulsion and explored capabilities of the nanoparticles (NPs) for A1AT encapsulation. Drug release profile from chitosan-genipin NPs (CS-GNP) was examined on simulated lung fluids (SLF) such as artificial lysosomal fluid (ALF) (pH 4.5) and Gamble's solution (pH 7.4). ALF is analogous to the fluid in which inhaled particles would come into contact after phagocytosis by alveolar and interstitial macrophages in the lung. Gamble's solution represents the interstitial fluid deep within the

lung. Application of simulated biological fluids can provide superior in sight of the release mechanisms and possible *in vivo* behavior (20). The aim of this work was to prepare a range of nanoparticle size using biocompatible and safe molecules as a carrier of A1AT to deposit in the deep lung.

## MATERIALS AND METHODS

### *Materials*

A1AT human plasma was obtained from Sigma-Aldrich (USA), chitosan (87% deacetylation) and genipin were purchased from Challenge Bioproducts (Taiwan). Hydroxypropyl- $\beta$ -cyclodextrin (HP- $\beta$ -CD) and triton X-100 were obtained from Sigma Aldrich (USA). Cyclohexane (98%), acetic acid (99.8%), hexanol were purchased from Merck (Germany). All other chemicals and reagents used were of analytical grade. All assays were performed in three separate experiments.

### *Preparation of chitosan-genipin nanohydrogel*

CS-GNP nanohydrogels were prepared according to the method reported by Pujana and coworkers (19), with insignificant modifications. Briefly, NPs were synthesized in two microemulsions including chitosan microemulsion (MC) and genipin microemulsion (MG). For preparation of MC and MG, at first aqueous solutions of chitosan and genipin were prepared by separately dissolving 1 g of chitosan or 1 g of genipin in 100 and 540 ml of 1% v/v aqueous acetic acid solution, respectively. Aqueous solutions of chitosan were sonicated using a probe type sonifier (Ultrasonic Homogenizer HU-600) at 60W for 20 min in an ice-cooled bath. Then cyclohexane and n-hexanol were mixed with either chitosan or genipin aqueous solutions separately in a flask at a fixed ratio of 2.75:1:1 (v/v). Finally, for microemulsion formation TritonX-100 was added drop wise into each solution while was vigorously stirring to become transparent. Then MC and MG were mixed by magnetic stirring. NPs were separated from microemulsion by ethanol precipitation process. The hardened NPs were collected by centrifugation at 30000 rpm for 30 min and washed three times with sterile

deionized water and ethanol. Finally, nanohydrogels were freeze-dried using 2.5% trehalose dihydrate as the cryoprotectant.

#### **Ultraviolet visible spectroscopy**

The chitosan-genipin cross-linking reaction was characterized by UV-Visible Spectroscopy Analysis ((Shimadzu, UV-3100, Japan). During the cross-linking reaction, spectra were obtained at certain time intervals in a wavelength range from 200 to 800.

#### **Fourier transform infrared spectroscopy**

For fourier transform infrared (FTIR) analysis of chitosan and CS-GNP nanohydrogels, 2 mg of each sample was milled with 100 mg of potassium bromide to form a fine powder. Subsequently, the powder was compressed into a thin pellet which was analyzed using Thermo Nicolet Nexus 670 FT-IR E.S.P.

#### **Transmission electron microscopy**

The morphology and size of the prepared CS-GNP nanohydrogels were characterized by Hitachi-7600 transmission electron microscopy (TEM) at an accelerating voltage of 40 kV. Samples were prepared by depositing a drop of CS-GNPNPs suspension on a copper grid fitted with a carbon support film and dried under vacuum.

#### **Zeta potential measurement**

The zeta potential of nanohydrogels solutions was measured with a zeta potential analyzer (Malvern Instruments, UK) at pH of 4 and 7.4.

#### **Swelling properties**

The swelling behavior of the dried hydrogel NPs was determined by swelling test using phosphate buffered saline (PBS) solutions with different pH (4, 7.5, and 12).

Dried test sample (50 mg) was immersed in swelling medium and incubated for 2 h at room temperature. At different time intervals, the swollen samples were removed from solutions and were blotted with a filter paper to eliminate the extra buffer on the surface. The swollen samples were weighed and the percentage of equilibrium water uptake was calculated as follows:

$$\text{Water uptake (\%)} = [(W_s - W) / W] \times 100 \quad (1)$$

where,  $W_s$  is the weight of the swollen hydrogel NPs and  $W$  is the initial weight of hydrogel NPs (14,21).

#### **Determination of particle size distribution**

Measurement of particle mean diameter and distribution of swollen CS-GNP nanohydrogels were performed using Laser light scattering (LLS) technique (Sem-633, Sematech, France). Samples were prepared by suspending 5mg of each sample in 5 ml of sterile deionized water and sonicated at amplitude of 40 and 0.5 s pulse cycle for 5 min (Ultrasonic Homogenizer HU-600).

#### **Bradford assay**

Protein quantification assays were performed using Bradford methods (BioRad Laboratories, Hercules, CA, USA). The Bradford assay is a direct method for protein quantification; Coomassie Brilliant Blue G-250 dye binds to aromatic and basic amino acid residues in proteins and the resulting complex absorbs at 595 nm. Standard curves were constructed using bovine serum albumin (BSA) (0.1–1 mg/ml final concentration) in dH<sub>2</sub>O. Microplate assays for method was performed according to manufacturer's recommendations and absorbance was measured on a microplate reader SUNRISE (Tecan, Crailsheim, Germany).

#### **Alpha-1 antitrypsin encapsulation on nanohydrogel**

For encapsulation of A1AT on dried hydrogel NPs, 200 mg of CS-GNP NPs was dispersed in 6 ml of PBS solution while sonicating at pH 7.4 at room temperature. 0, 1, 2, 3 mg of A1AT was dissolved in 0.5 ml of citrate buffer (pH 8) containing 5% (2-hydroxypropyl)- $\beta$ -cyclodextrin, which has been reported to decrease loss of protein activity in water phase (22). Protein solutions were added to PBS solution containing CS-GNP NPs. The samples were then placed for 24 h on a rotating agitator at room temperature for 24 h. Loaded NPs were collected by centrifugation at 20,000 rpm for 45 min. Supernatant was carefully decanted and protein content in the supernatant was measured spectrophotometrically at 595 nm

using the Bradford method. Intrinsic absorption of the samples was removed by a calibration curve using PBS solution containing 0.5 ml of citrate buffer (pH=8), 5% (2-hydroxypropyl)- $\beta$ -cyclodextrinan and non-loaded hydrogel NPs. At each time interval, the A1AT encapsulation efficiency (EE) was calculated using following equation (23):

$$EE (\%) = (C_0 - C_1) / C_0 \times 100 \quad (2)$$

where,  $C_0$  is total amount of A1AT and  $C_1$  is free amount of A1AT in the supernatant.

### ***Evaluation of drug release profile in pseudo alveolar fluid***

*In vitro* drug release from loaded CS-GNP NPs was measured in SLFs (20). To study the effect of initial protein concentration on drug release, dried test samples loaded with various initial protein concentrations (0, 1, 2, 3 mg/ml) were immersed in 6 ml of Gamble's solution. Also, effect of different pH (4.5 and 7.4) on A1AT release profile in Gamble's solution and ALF was investigated with dried NPs loaded with 3 mg/ml initial protein concentration. Finally, drug release profile in Gamble's solution was compared with saline solution at pH 7.4.

All samples were incubated in a water bath at 37 °C for 24 h. At different time intervals, 1 ml of each solution was withdrawn and replaced with the equal volume of similar fresh solutions. Aliquots were centrifuged at 20000 rpm for 20 min to precipitated NPs and then protein concentration of the supernatants was measured with Bradford method. A calibration curve was generated at each time interval using NPs without A1AT loaded to correct for the intrinsic absorbance of NPs that

may not precipitated with centrifugation (24,25).

### ***Drug bioactivity after release from NPs***

The antitryptic proteins (such as A1AT) inhibit the hydrolysis of N-benzoyl-DL-arginine-p-nitroanilide by trypsin present in Tris buffer. The reaction was stopped by adding acetic acid, and the absorbance is then read at 400 nm. In this study, A1AT activity after release from NPs was determined by trypsin inhibitory capacity (TIC) assay according to the method reported by Albert A. Dietz and colleagues (26). At different time intervals, TIC for released A1AT from NPs was compared with equal amount of free A1AT as a control.

## **RESULTS**

### ***Ultraviolet visible spectroscopy analysis***

The reaction mechanism for the synthesis of CS-GNP network includes two responds. At first, the carboxymethyl group of genipin reacts with amino group of chitosan to form secondary amide. Subsequently, nucleophilic attack occurs on olefinic carbon atom at C-3 of deoxylognaninaglycone by amino group of chitosan which is followed by the opening of the dihydropyran ring to form heterocyclic amine. The reaction was confirmed by UV spectral analysis (Fig. 1). As showed in Fig. 1, maximum absorption peak at 240 nm decreased at the end of the first day. It was attributed to formation amid linkage due to nucleophilic attack of amine group to ester groups on genipin and formation of new peak at 290 nm belong to heterocyclic CS-GNP nanohydrogel formation (27).

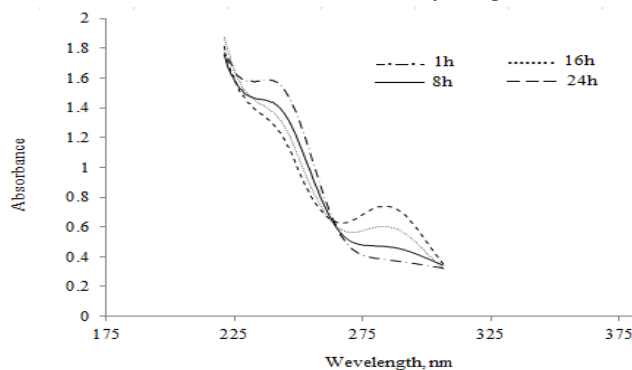


**Fig. 1.** The UV spectra analysis of chitosan cross linking with genipin during 24 h period.

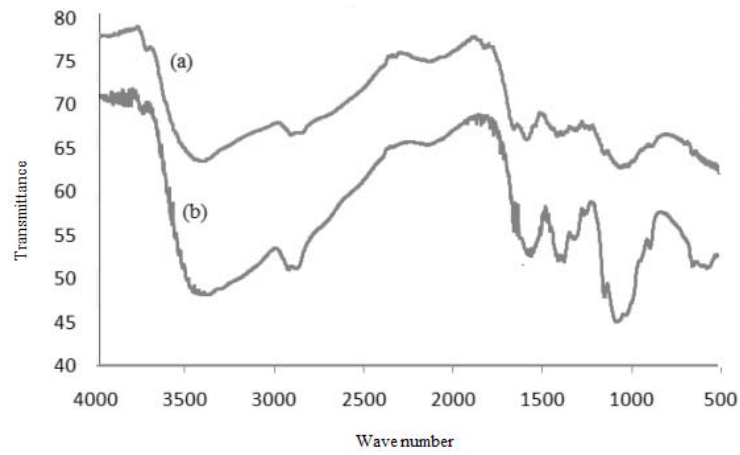


**Fig. 2.** The FTIR spectra of dry powder of: a;chitosan before cross linking with genipin and b;chitosan after cross linking with genipin solution (CS-GNP nanohydrogel).

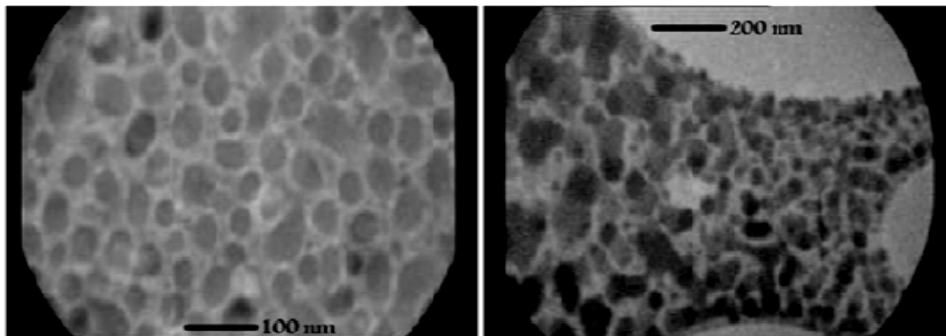


**Fig. 3.** Transmission electron microscopy micrographs of CS-GNP nanoparticles.

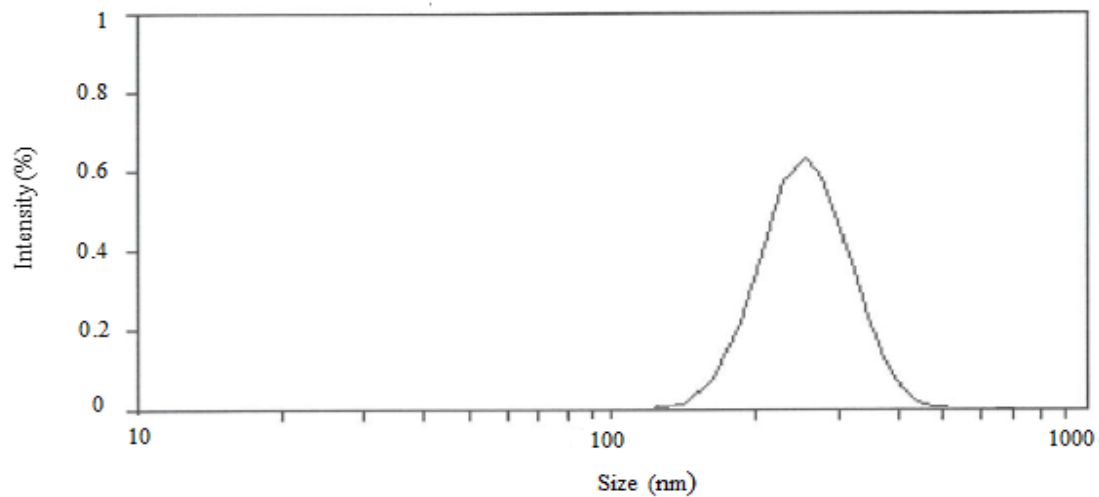


**Fig. 4.** Size and distribution of CS-GNP nanoparticles determined by laser light scattering (LLS).

### **Fourier transform infrared spectral analysis**

The formation of a complex between chitosan and genipin inspected in the solid samples by transmission FTIR spectroscopy. Fig. 2 shows FTIR spectra recorded for KBr pellets of a chitosan control and CS-GNP complex (Spectrum b). According to this figure, there are only subtle differences between the two spectra.

The intensity of amide bands at  $1560\text{ cm}^{-1}$  was increased revealing that the carboxymethyl group of genipin reacted to amino group to form secondary amide. The newly formed broad peak at  $1300\text{ cm}^{-1}\sim 1500\text{ cm}^{-1}$  suggests the presence of heterocyclic amine ring-stretching, which formed to nucleophilic attack by amino group of chitosan on the olefinic carbon atom at C-3 of deoxyloguaninaglycone.

These were followed by the opening of the dihydropyran ring to form heterocyclic amine. Two spectrum presented characteristic absorption bands at  $3100\text{-}3350\text{ cm}^{-1}$ , and  $1100\text{ cm}^{-1}$  which correspond to  $\text{-OH}$ ,  $\text{C-O}$  stretching, respectively. Finally, FTIR results confirmed the formation of cross-linked networks with short chains of cross-linking bridges (14,27).

### **Particle size and distribution**

Electron microscopy analysis confirmed the presence of NPs and provided morphological information of the dried CS-GNP NPs. With TEM, particles were detected in spherical, distinct and regular shapes with mean particle size ranged from 30 to 100 nm in dried form (Fig. 3). The NPs did not show a smooth surface but a fluffy appearance. Also, the LLS results shows that NPs were detected as dispersed and homogenize entities (Fig. 4). It is noteworthy that the diameter of the CS-GNP NPs measured by LLS was significantly higher than those estimated from microscopy particularly because of the high swelling capacity of CS-GNP NPs.

### **Zeta Potential**

Zeta potential of CS-GNP nanohydrogels can greatly influence their stability in suspension by means of electrostatic repulsion between the particles. Our results

demonstrated that zeta potentials of CS-GNP NPs at pH 4 and 7.4 were  $27.3 \pm 2.5$  and  $8.1 \pm 3.1$  mV, respectively. The higher zeta potential in acidic pH could be related to the ionization of free amine groups of chitosan backbone, which results in the electrostatic repulsion.

### **Swelling degree**

Swelling measurements were performed on CS-GNP NPs without drug loading. Fig. 5 illustrates the degree of swelling of CS-GNP hydrogels in media with different pH. The water uptake at pH 9 was lower than those of other conditions. At pH 7.5, water uptake was higher than that of pH 12. The highest water uptake was observed under acidic condition at pH 4. Thus, the water uptake by CS-GNP hydrogel NPs was increased as the pH of surrounding buffer solution was decreased.

### **Encapsulation efficiency**

The EEs of CS-GNP hydrogel NPs in PBS solutions with initial A1AT concentrations of 1, 2 and 3 mg/ml were measured to be  $80 \pm 1.8\%$ ,  $86 \pm 2.1\%$  and  $90 \pm 2.6\%$ , respectively. It is obvious that the EE tended to increase concentration dependently.

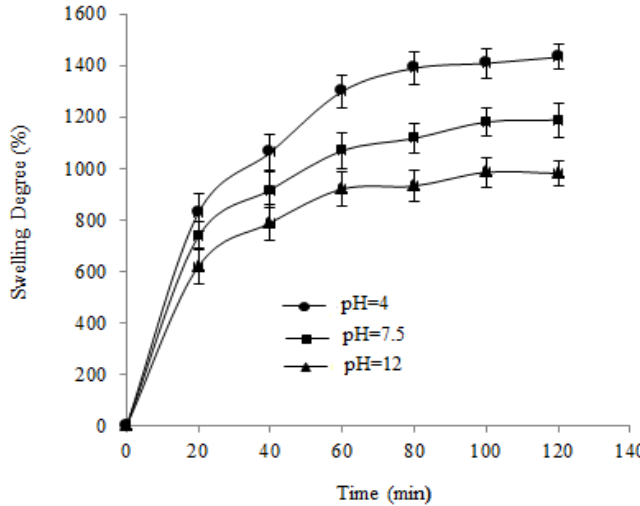
### **Cumulative Alpha 1- antitrypsin release**

Fig. 6 shows the sustained release behavior of A1AT from CS-GNP hydrogel NPs containing different amounts of protein in Gamble's solution over a 12-day period. As shown in Fig. 6, the protein release rate depends on A1AT loading content. Therefore, increase of A1AT loading in NPs, led to a higher release rate of the drug from hydrogels. Fig. 7 shows the cumulative release profile of A1AT from CS-GNP hydrogel NPs in Gamble's solution with pH 7.4 and ALF with pH 4.5 as a function of time. It can be seen that about 60% of protein was released from NPs at pH of 4.5 and 44% at pH 7.4 within 12-day period. The increased release rate of the protein from CS-GNP hydrogel NPs incubated in the low pH media is likely due to the reduced interactions between the proteins with NPs. As demonstrated in Fig. 8, cumulative release of A1AT into pseudo alveolar fluid was more than that of saline solution as a control media.

**Bioactivity of released Alpha 1- antitrypsin from nanoparticles**

To investigate the bioactivity of A1AT after release from NPs, TIC of released A1AT from NPs was detected in comparison to free A1AT

as the control. As shown in Fig. 9, the activity of released A1AT from NPs was similar to that of control up to 72 h. However, bioactivity of released A1AT was significantly reduced after 72 h.



**Fig. 5.** Swelling behavior of CS-GNP nanohydrogel at various pH (4, 7.4, and 12) at 37 °C (Mean ± SD, n=3).

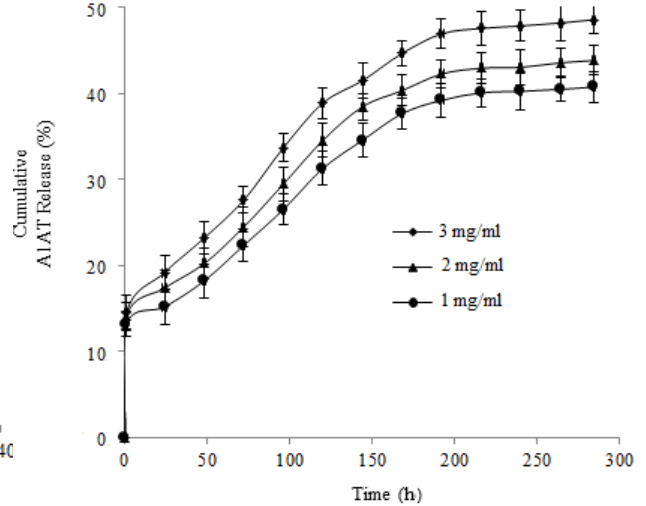


**Fig. 6.** Cumulative alpha 1-antitrypsin release from CS-GNP nanoparticles at different alpha 1-antitrypsin loading concentrations in Gamble’s solution (pH 7.4) at 37 °C during 12-day period. Data represents the mean ± SD, (n=3 per group).

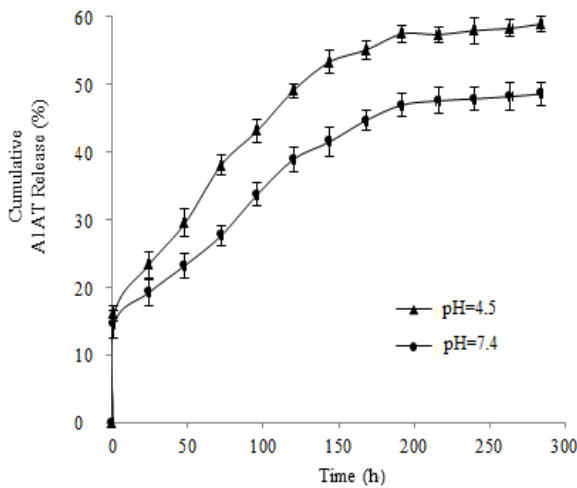


**Fig. 7.** Cumulative alpha 1-antitrypsin release profile from CS-GNP nanoparticles in Gamble’s solution (pH 7.4) and ALF (pH 4.5) at 37 °C during 12day period at 37 °C during (mean ± SD, n=3).

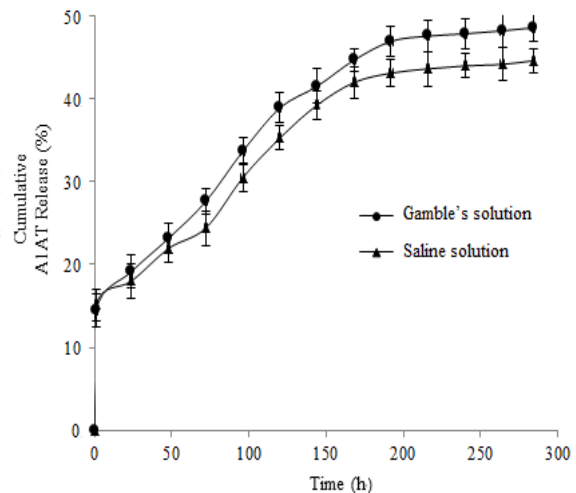


**Fig. 8.** Comparison of cumulative alpha 1-antitrypsin release profile from CS-GNP nanoparticles in Gamble’s solution as a pseudo alveolar fluid and saline solution as a control media at 37 °C during 12 day period (mean ± SD, n=3).

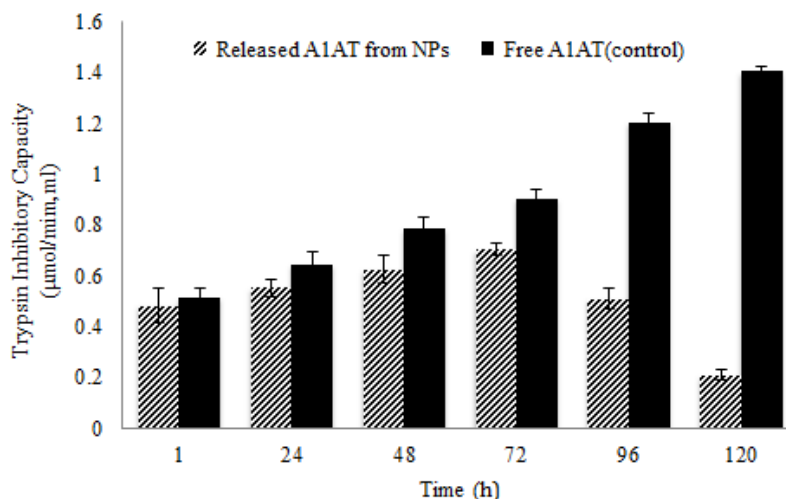


**Fig. 9.** Comparisons of trypsin inhibitory capacity of released A1AT from CS-GNP nanoparticles and free A1AT as a control. Data shown are the mean  $\pm$  SD (n=3).

## DISCUSSION

A1AT deficiency is a lethal hereditary disorder characterized by a severe diminution in plasma levels of A1AT. The recognition of A1AT deficiency as a cause of emphysema then led to what is still the prevailing theory for the pathogenesis of emphysema, the protease-anti-protease theory (2). A1AT inhibits a broad range of proteases and protects the lung from neutrophil elastase during inflammation or infection. The absence or inefficient function of A1AT in the lungs leads to uncontrolled function of elastase and elastin breakdown, resulting in respiratory problems such as COPD and emphysema. Therefore, only with appropriate and adequate concentrations of A1AT the lungs' normal function can be maintained (3). One of the possible treatment strategies is the delivery of the medications through respiratory system. This route offers many advantages such as noninvasive administration via inhalation aerosols, avoidance of first-pass metabolism, direct delivery to the site of action for the treatment of respiratory diseases, and the availability of a huge surface area for local drug action and systemic absorption of drugs. Colloidal drug delivery systems have extensively been investigated as drug carrier systems for the pulmonary delivery of drugs. Nanoparticulate drug delivery systems have opened new perspectives due to offering many

advantages such as increasing drug solubility, promotion of encapsulation efficiency, controlling drug release, reducing dosing frequency, uniform distribution of drug among the alveoli, efficient drug transport to the lung epithelium, and decreasing incidence of side effects. Therapeutically used polymeric NPs are composed of biodegradable or biocompatible materials, such as poly (lactic acid) (PLA), poly (lactic-co-glycolic acid) (PLGA), alginic acid, gelatin and chitosan (10,28,29). Chitosan is an attractive polymer as drug delivery carriers because of its biocompatibility, biodegradability and non-toxicity together with its antimicrobial activity and low immunogenicity. Chitosan has also been extensively used to enhance the intranasal delivery of therapeutic compounds (10,30).

Nanoparticles have been proposed as valuable vehicles for efficient drug transport to the lung epithelium while avoiding unwanted mucociliary clearance and phagocytic mechanisms. Recent studies on pulmonary nanoparticle deposition suggest that inhaled nanoparticles are the optimal particle size for alveolar deposition, as well as for minimizing the lung phagocytosis (31): It has been reported (32) that the DPI particles having a size ranged between 1  $\mu$ m to 5  $\mu$ m could be efficiently deposited in the lung tissues and the particles smaller than 260 nm are hardly phagocytized by macrophagocytes, which

leads to the bioactivities of the DPI particles in lung cells (33). In the current work, we prepared hydrogel NPs with size range of 30 to 100 nm. However, LLS results showed that hydrogel NP sizes are increased once absorbing water from dispersing medium and become swollen. Most of the hydrogel systems are responsive to pH variations of the immersion medium and therefore, the degree of swelling of the network changes under different pH conditions. Under acidic condition, the amino groups on chitosan polymer are protonated and electrostatic repulsion between the ionized amine groups ( $-NH_3^+$ ) results in an expansion of the network chains leading to an increase in swelling (14,34). Zeta potential measurements confirmed the progressive protonation of amino groups when the pH decreased.

EE is an important factor in the selection of carrier in drug delivery systems. Our results showed that the EE increased in the presence of higher initial concentrations of A1A1. In agreement with our findings, it has been reported that the increase in initial BSA concentration during encapsulation process increased the EE of the protein (23). The same trend was also reported by Berthold and coworkers for anti-inflammatory drugs (35). In contrast, other studies have shown the reverse effect of initial protein concentrations on protein encapsulation. Xu and Du reported that loading efficiency was decreased once BSA concentration increased at pH 6.0 (24). On the other hand, Akbuga and Bergisadi observed that the protein concentration had no effect on the EE of cisplatin (36). In the present study, A1AT loading was carried out by protein adsorption on nanoparticle surface with electrostatic interaction and direct entrapment into the polymer matrix. No cross-linker molecules were used to bind A1AT on the chitosan polymer. Encapsulation may also be affected by decreasing the size of NPs that result in higher surface to volume ratio which provides larger surface area for attachment of protein to NPs.

A1AT showed a sustained release profile from CS-GNP hydrogel NPs. However, in the first hours of release, NPs loaded with A1AT at concentrations of 1-3 mg/ml exhibited initial

burst release of 13-15%. Over a 12-day period, the cumulative protein release from NPs loaded with A1AT at a concentration of 3 mg/ml was yet maintained at approximately 45%. This is because some protein molecules might have been cross-linked with the hydrogel network or entered the NPs core which cannot be released unless polymer matrices are degraded. Higher release of A1AT from NPs with higher drug contents seemed to attribute to the higher protein concentration gradient between the polymer and release medium, which produced a higher diffusion rate (24,37,38). In agreement with our study on testing the effect of protein loading concentrations on protein release from NPs, Bhattarai and colleagues has shown that by increasing BSA loading concentrations the protein release rates was increased (39). Also, Wu and coworkers have shown that insulin release depended on the rate of diffusion to loading amount of protein (40).

The main target tissue of A1AT is the lungs, where released drug must perform its anti-protease activity locally and become absorbed efficiently by the lung epithelial membrane to provide appropriate concentrations of the anti-protease in the interstitial space and blood for further support. Therefore, the amount of drug to be released must be in proportion to the severity of protein deficiency in a specific period of time. A1AT threshold concentration is 11  $\mu$ M in circulation (25,41). Thus, this level can be expected as a protective concentration for the lungs against protease invasions. At a specific period of time, drug delivery systems for A1AT must provide the threshold concentration in a range that does not impair the function of human lung cells, such as the alveolar epithelial and endothelial cells. In the release experiment, it seems that the amount of A1AT released from CS-GNP hydrogel NPs over 12-day period could result in concentration below A1AT threshold *in vivo*. However, to obtain optimum A1AT release and concentration, besides initial concentration of A1AT to obtain desirable loading amount, the quantity of particles carrying proteins can be optimized. Furthermore, our findings suggest that the drug release properties of CS-GNP hydrogel

NPs are pH dependent. The results also showed lower A1AT release from NPs exposed to Gamble's solution at pH 7.4 compared to ALF at pH 4.5 which is probably due to the reduced electrostatic interactions between the A1AT and NPs at pH 4.5. Hence, pH dependent release of A1AT from CS-GNP hydrogel NPs should be considered once applied into the lung under various clinical conditions.

The effects of lungs fluid components such as inorganic salts, chlorides, carbonates, and phosphates of alkaline and alkaline earth metals on drug release profile evaluated through a comparison between A1AT release profile in Gamble's solution as a pseudo alveolar fluid and saline solution as a control media. Cumulative release of A1AT into pseudo alveolar fluid was higher than its release in saline solution. These results may be attributed to the reduced interactions between NPs and A1AT due to competition of lung fluid components with protein to associate with NPs. Because electrostatic interactions were found to be important for drug encapsulation, we hypothesized that electrostatic interaction could also influence drug release from nanoparticles. Cationic polymers such as chitosan, owing to their high negative-charge density can bind substantial amounts of negative charges on proteins. Since the initial binding of drug to the polymer is predominantly based on electrostatic complementarity, increased ionic strength, to some extent, helps in mitigating the electrostatic attraction, resulting in less effective binding and hence relatively faster dissociation of drug from drug/polymer complex although further studies are needed to confirm these results (42). Our results on A1AT activity after release from NPs revealed that polymer matrix does not affect A1AT activity. Decrease in protein bioactivity after 72 h may be due protein aggregation in NPs surface. Nanoparticles provide surface charges to promote the adherence of proteins, and their large surface area provides the potential to induce protein aggregation (43). Finally, our data shows that this drug delivery system for A1AT delivery to the lung has the potential for further evaluation *in vivo*.

## CONCLUSION

The CS-GNP NPs were prepared with nontoxic and biocompatible molecules using emulsification-cross-linking method for pulmonary drug delivery of A1AT. The size of NPs is appropriate to be deposited in respiratory region of the lung and to be protected from phagocytosis by lung macrophages. Swelling properties of the NPs could be controlled by environment factors such as pH which affects drug lease and loading. Drug release behavior depended on the initial drug concentration at loading time, pH variations and components of release media. The data presented in this study confirmed that the drug carrier designed can be a potential therapeutic strategy in cargo delivery to the lung.

## ACKNOWLEDGMENTS

We would like to appreciate Mr. Saied Sepehri for his technical support in conducting TEM analyses.

## REFERENCES

1. Huber R, Carrell RW. Implications of the three-dimensional structure of alpha 1-antitrypsin for structure and function of serpins. *Biochemistry*. 1989;28:8951-8966.
2. Mulgrew AT, Taggart CC, McElvane NG. Alpha-1-antitrypsin deficiency: current concepts. *Lung*. 2007;185:191-201.
3. Kalsheker N. Alpha 1-antitrypsin: structure, function and molecular biology of the gene. *Biosci Rep*. 1989;9:129-138.
4. Chotirmall SH, Carroll T, SpoooneM, McElvaney NG. Priorities for the alpha-1 community: The physician's perspective. *Pharma Policy Law*. 2009;11:285-297.
5. Wood AM, Stockley RA. Perspective Alpha one antitrypsin deficiency: from gen to treatment. *Respiration*. 2007;74:481-492.
6. Scott LJ, Evansm EL, Dawes PT, Russell GI, Matthey DL. Comparison of IgA alpha1-antitrypsin levels in rheumatoid arthritis and seronegativeoligoarthritis: complex formation is not associated with inflammation per se. *Br J Rheumatol*. 1998;37:398-404.
7. Smola M, Vandamme T, Sokolowski A. Nanocarriers as pulmonary drug delivery systems to treat and to diagnose respiratory and non-respiratory diseases. *Int J nanomedicine*. 2008;3:1-19.

8. Hoet PH, Brüske-Hohlfeld I, Salata OV. Nanoparticles—known and unknown health risks. *J Nanobiotechnology*. 2004;2:12.
9. Berger J, Reist M, Mayer JM, Felt O, Peppas NA, Gurny R. Structure and interactions in covalently and ionically cross-linked Chitosan hydrogels for biomedical applications. *Eur J Pharm Biopharm*. 2004;57:19–34.
10. Ding J, Na L, Mao S. Chitosan and its derivatives as the carrier for intranasal drug delivery. *Asian J of Pharm Sci*. 2012;7:349–361.
11. Muzzarelli RAA. Genipin-cross-linked chitosan hydrogel as biomedical and pharmaceutical aids. *Carbohydr Polym*. 2009;77:1–9.
12. Hamidi M, Azadi A, Rafiei P. Hydrogel nanoparticles in drug delivery. *Adv Drug Deliv Rev*. 2008;60:1638–1649.
13. Ruvalcaba AM, Díaz JC, Becerra F, CBarba LE, Álvarez AG. Swelling characterization and drug delivery kinetics of polyacryl amide-co-itaconic acid/Chitosan hydrogels. *eXPRESS Polym Lett*. 2009;3:25–32.
14. Chen S C, Wu YC, Mi FL, Lin YH, Yu LC, Sung HW. A novel PH-sensitive hydrogel composed of N, O- carboxymethyl Chitosan and alginate cross-linked by Genipin for protein drug delivery. *J Control Release*. 2004;96:285–300.
15. Zhi J, Wang YJ, Luo GS. Adsorption of diuretic furosemide on to Chitosan nanoparticles prepared with a water-in-oil nanoemulsion system. *React Funct Polym*. 2005;65:249–257.
16. Tsai ML, Bai SW, Chen RH. Cavitation effects versus stretch effects resulted in different size and polydispersity of ion tropic gelation Chitosan-sodium tripolyphosphate nanoparticle. *Carbohydr Polym*. 2008;71:448–457.
17. Harris R, Lecumberri E, Heras A. Chitosan-genipin microspheres for the controlled release of drugs: clarithromycin, tramadol and heparin. *Mar Drugs*. 2010;8:1750–1762.
18. Chiou SH, Hung TC, Giridhar R, Wu WT. Immobilization of lipase beads using a natural cross-linker. *Prep Biochem Biotechnol*. 2007;37:265–275.
19. Pujana MA, Álvarez LP, Iturbe LCC, Katime, I. Water soluble folate-chitosan nanogels cross-linked by genipin. *Carbohydr Polym*. 2014;101:113–120.
20. Marques MRC, Loebenberg R, Almukainzi M. Simulated biological fluids with possible application in dissolution testing. *Dissolut Technol*. 2011;18:15–28.
21. Liu J, Zhang SM, Chen PP, Cheng L, Zhou W, Tang WX, *et al*. Controlled release of insulin from PLGA nanoparticles embedded within PVA hydrogels. *J Mater Sci: Mater Med*. 2007;18:2205–2210.
22. Kang F, Jiang G, Hinderliter A, DeLuca PP, Singh J. Lysozyme stability in primary emulsion for PLGA microsphere preparation: effect of recovery methods and stabilizing excipients. *Pharm Res*. 2002;19:629–633.
23. Gan Q, Wang T. Chitosan nanoparticle as protein delivery carrier—systematic examination of fabrication conditions for efficient loading and release. *Colloids Surf B Biointerfaces*. 2007;59:24–34.
24. Xu Y, Du Y. Effect of molecular structure of chitosan on protein delivery properties of chitosan nanoparticles. *Int J Pharm*. 2003;250:215–226.
25. Brantly ML, Wittes JT, Vogelmeier CF, Hubbard RC, Fells GA, Crystal RG. Use of a highly purified  $\alpha$ 1-antitrypsin standard to establish ranges for the common normal and deficient  $\alpha$ 1-antitrypsin phenotypes. *Chest*. 1991;100:703–708.
26. Dietz AA, Rubinstein HM, Hodges L. Measurement of  $\alpha$ -1-Antitrypsin in serum, by immunodiffusion and by enzymatic assay. *Clin Chem*. 1974;20:396–399.
27. Mi FL, Sung H. Synthesis and characterization of a novel Chitosan-based network prepared using naturally occurring cross linker. *J polymer Sci part A: Polym Chem*. 2000;38:2804–2814.
28. Mansour HM, Rhee YS, Wu X. Nanomedicine in pulmonary delivery. *Int J Nanomedicine*. 2009;4:299–319.
29. Paranjpe M, Müller-Goymann CC. Nanoparticle-mediated pulmonary drug delivery: a review. *Int J Mol Sci*. 2014;15:5852–5873.
30. Liu Y, Ibricevic A, Cohen JA, Gunsten SP, Frechet JM, *et al*. Impact of hydrogel nanoparticle size and functionalization on *in vivo* behavior for lung imaging and therapeutics. *Molecular pharmaceutics*. 2009;6:1891–1902.
31. Hoet P, Bruske-Hohlfeld I, Salata OV. Nanoparticles, known and unknown health risks. *J Nanobiotechnol* 2004;2:1–15.
32. Niven RW. Recent advances in liposomal dry powder formulations: preparation and evaluation. *Crit Rev Ther Drug Carr Syst*. 1995;12:151–231.
33. Bosquillon C, Lombry C, Preat V, Vanbever R. Characterization and aerosol dispersion performance of spray-dried chemotherapeutic PEGylated phospholipid particles for dry powder inhalation delivery in lung cancer. *J Control Release*. 2001;70:329–339.
34. Tanuma H, Saito T, Nishikawa K, Dong T, Yazawa K, Inoue Y. Preparation and characterization of PEG-cross-linked chitosan hydrogel films with controllable swelling and enzymatic degradation behavior. *Carbohydr Polym*. 2010;80:260–265.
35. Berthold A, Cremer K, Kreuter J. Preparation and characterization of chitosan microspheres as drug carrier for prednisolone sodium phosphate as model for anti-inflammatory drugs. *J Control Release*. 1996;36:17–25.
36. Akbuga J, Bergisadi N. Effect of formulation variables on cis-platin loaded chitosan microsphere properties. *J Microencapsulation*. 1999;16:697–703.
37. Janes KA, Calvo P, Alonso MJ. Polysaccharide colloidal particles as delivery systems for macromolecules. *Adv Drug Deliv Rev*. 2001;47:83–97.
38. Miyazaki S, Yamaguchi H, Yokouchi C, Takada M, Hou WM. Sustained-release of indomethacin from chitosan granules in beagle dogs. *J Pharm Pharmacol*. 1988;40:642–643.

39. Bhattarai N, Ramay HR, Chou SH, Zhang M. Chitosan and lactic acid-grafted chitosan nanoparticles as carriers for prolonged drug delivery. *Int J of Nanomedicine*. 2006;1:181–187.
40. Wu ZM, Zhang XG, Zheng C, Li CX, Zhang SM, Dong RN, *et al.* Disulfide-cross-linked chitosan hydrogel for cell viability and controlled protein release. *Eur J Pharm Sci*. 2009;37:198–206.
41. Buist AS, Burrows B, Cohen A, Crystal RG, Fallat RJ, Gadek JE, *et al.* Guidelines for the approach to the patient with severe hereditary alpha-1-antitrypsin deficiency. *Am Rev Respir Dis*. 1989;140:1494-1497.
42. Manocha B, Argyrios M. Controlled release of doxorubicin from doxorubicin/ $\gamma$ -polyglutamic acid ionic Complex. *J Nanomater*. 2010;2010:1-9.
43. Zaman M, Ahmad E, Qadeer AI, Rabbani G, Khan RH. Nanoparticles in relation to peptide and protein aggregation. *Int J Nanomedicine*. 2014;9:899–912.